



EARTHQUAKE RELIABILITY OF STRUCTURES

Asadour HADJIAN^{1,2}

SUMMARY

The current treatment of the reliability of structures under earthquake loads is at best heuristic. A design to a specific scenario event or a specific return period ground motion intensity does not address the earthquake reliability of the resulting structure. This is so simply because any one structure is potentially exposed, throughout its design life, to *all* the possibilities of the occurrence of ground motion intensities at a given site as characterized by a set of site-specific seismic hazard curves (mean, median, and several specified exceedance percentiles). The use of this complete hazard information is prerequisite to estimating earthquake “failure” probabilities. “Failure” is a generic term defining non-performance at a preselected limit state. In order that all pairs of ground motion intensities and associated exceedance probabilities are considered, the site hazard curves are substituted by the median curve and an across-variability parameter, ζ_H . First, the *conditional* (given that median load level \check{a} occurs) failure probability curve is calculated by the convolution of the load and resistance distribution functions. It is demonstrated that both the load and resistance can be idealized as lognormally distributed functions with logarithmic standard deviations ζ_H and ζ_R , respectively, where ζ_R incorporates the variabilities in response modeling, response calculations, material variabilities and design equations. To calculate the *unconditional* failure probability, P_F , each conditional failure probability is multiplied by the corresponding probability of the occurrence of \check{a} , and then summed over all occurrences of \check{a} . The resulting integral is transformed into an algebraic relation by making a simple assumption on the local behavior of the median hazard curve. Design parameters affecting P_F are explored. Randomness and uncertainty issues are discussed. The across-variability parameter, ζ_H , has a significant impact on reliability, and must be explicitly included in design.

INTRODUCTION

Building design codes achieve a preselected reliability by the use of partial load and capacity reduction factors. Although the determination of these factors, say for dead and live loads, is rooted in basic reliability concepts, the reliability of structures subjected to earthquake loads is not determined as

¹Tech Staff, Defense Nuclear Facilities Safety Board, Washington DC. E-mail: asadourh@dnfsb.gov

²**Disclaimer:** The views expressed in this paper are solely those of the author, and no endorsement of the paper by the Defense Nuclear Facilities Safety Board is intended nor should be inferred.

explicitly. Designing structures to specific scenario events or return periods of earthquake ground motion parameters, such as those proposed in Table 1 [1], does not address the earthquake reliability of the resulting structures, except maybe heuristically. This is so simply because any structure is potentially exposed to *all* ground motion occurrences varying from very small to very large return periods. And therefore, to estimate the earthquake “failure” probability, where “failure” is a generic term defining

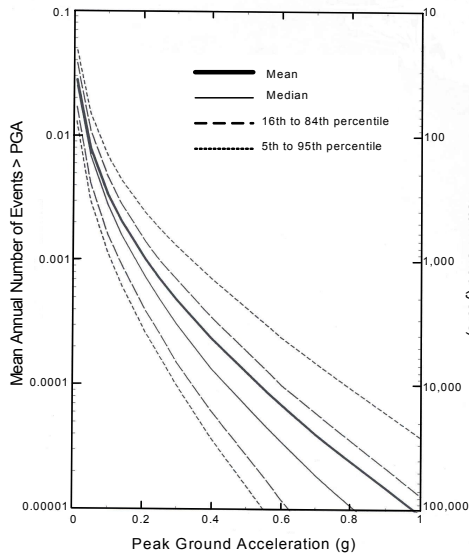
Table 1. Vision 2000 performance objectives (Poland [1])

Limit State- ↓ Ground Motion	Fully Operational	Functional	Life Safety	Near Collapse
Frequent 50% in 50 yrs ~75 yrs RP	S			
Occasional 20% in 50 yrs ~225 yrs RP	E	S		
Rare 10% in 50 yrs ~500 yrs RP	C	E	S	
Very Rare* 5% in 50 yrs ~1000 yrs RP	N/A	C	E	S

non-performance at any preselected limit state, all ground motion intensities with associated exceedance probabilities must be considered. Thus, the first step in calculating the earthquake reliability of structures is the complete characterization of the site seismic hazard, and not just a single point on the mean hazard curve.

*FEMA 273 (1997) specifies a 2% in 50 yrs exceedance probability (~2500 years mean return period).

GENERALIZED EARTHQUAKE HAZARD



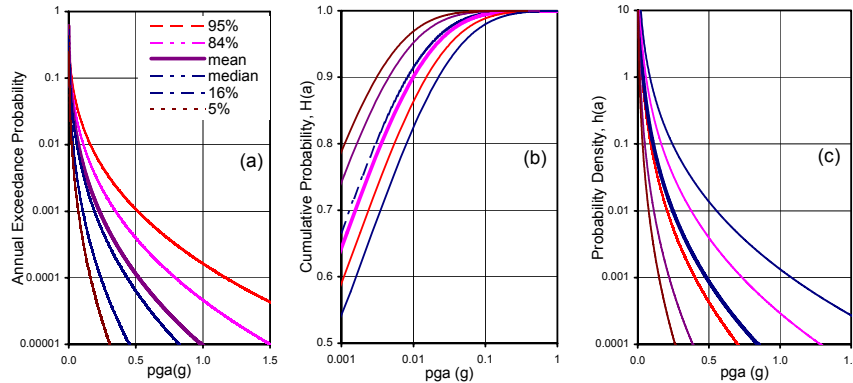
As shown in Figure 1, earthquake hazard is usually characterized by curves relating the exceedance probability of a ground motion parameter to the intensity level of the ground motion variable. Throughout this paper peak ground acceleration (pga) is used for demonstration purposes; other ground motion parameters, such as spectral acceleration or displacement, could as well be used. Given the significant uncertainties in ground motion estimates, a proper probabilistic seismic hazard evaluation includes the variability of the selected ground motion parameter at all exceedance probabilities. This uncertainty is characterized in Figure 1 by several hazard curves at preselected percentiles. For the basic elements of calculating seismic hazard curves see SSHAC [2]. A hazard curve, $\hat{H}(a)$, is the complementary cumulative distribution function of the selected ground motion parameter. The Cumulative Distribution Function (CDF) of the hazard,

Figure 1. Example of mean, median and four selected percentile curves for characterizing pga seismic hazard

$H(a)$, is simply $[1 - \hat{H}(a)]$. Thus, the Probability Density Function (PDF) of the hazard is given by

$$h(a) = \frac{dH(a)}{da} = \frac{d [1 - \hat{H}(a)]}{da} = -\frac{d\hat{H}(a)}{da} \quad (1)$$

Figure 2a shows a set of idealized hazard curves. Based on the above relation, the CDF and the PDF of

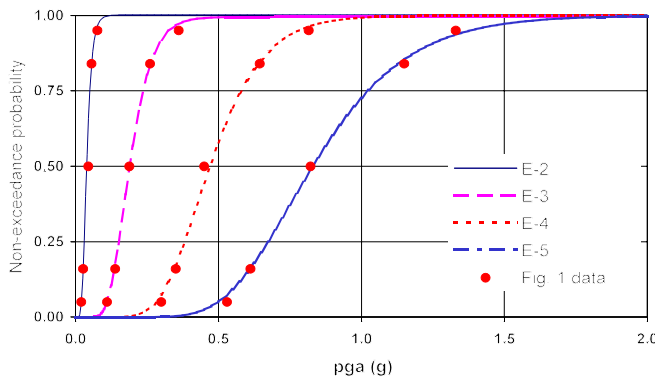


the hazard curves of Figure 2a are calculated and shown in Figures 2b and 2c, respectively. From Figure 2a the median pga for any exceedance probability can be read off. For example, the median pga at the 2500 year return period (exceedance probability of 4×10^{-4} or 2% in 50 years) is 0.27g and for 10,000 year return period (exceedance probability of 10^{-4} or 0.5% in 50 years) is 0.44g.

Figure 2. Idealized seismic hazard curves for several percentiles based on $\zeta_H=0.6$: (a) hazard curves, (b) CDFs and (c) PDFs

Across-variability

Returning to Figure 1 it is noted that the pga at any exceedance probability varies by more than a factor of two, reflecting the uncertainties in estimating ground motion. This uncertainty must be somehow quantified for use in failure probability analysis. The probability distribution of the pga at any



exceedance probability can be approximated based on the percentile data. Data points at four selected exceedance probabilities are plotted in Figure 3 (dots). Also shown are plots of idealized lognormal CDF curves. Based on physical attributes of the problem and mathematical expedience, the use of the lognormal distribution has become the distribution of choice for similar seismic probabilistic assessments [3]. Given empirical data, the lognormal distribution parameters, ζ_H and λ_{H_p} , can be estimated from plots of the data points on lognormal probability paper. For details of this procedure see Ang and Tang [4].

Figure 3. Idealization of the across-variability of Figure 1 data points as lognormal distributions

Results and data from Figure 3 are tabulated in Table 2 for the four selected exceedance probabilities. Note that the idealized lognormal distributions adequately estimate the medians but underestimate the means. Nevertheless, the comparison shown in Figure 3 of the idealized distributions with the data points from Figure 1, suggests that, overall, the lognormal representation of the across-variability of hazard curves is possible. Of significance is the possibility of characterizing the dispersion of the ground motion with a single ζ_H at all exceedance probability levels. These encouraging results should not be surprising. Hazard curves are generated by a series of multiplications, and hence, based on the central limit theorem, a lognormal distribution is expected regardless of the distribution of the independent parameters (Ang and Tang [5]). In the following derivations, it is assumed that the ζ_H are identically the same at all exceedance probabilities. In effect, this across-variability parameter, ζ_H , together with the median curve are a substitute for the complete set of hazard curves such as in Figures 1 and 2.

Table 2. Across-variability parameters at four exceedance probabilities

Exceedance Probability	E-2	E-3	E-4	E-5
ζ_H (probability paper)	0.38	0.32	0.31	0.31
λ_H (probability paper)	-3.26	-1.67	-0.76	-0.19
Estimated a_{50} (g) [$x_{50}=e^\lambda$]	0.039	0.19	0.47	0.83
a_{50} from Figure 1	0.044	0.19	0.45	0.82
Estimate to actual ratio (%)	89	100	104	101
Estimated \bar{a} (g) [$\mu=x_{50}\exp(\frac{\zeta^2}{2})$]	0.041	0.20	0.49	0.87
\bar{a} from Figure 1	0.045	0.22	0.56	1.03
Estimate to actual ratio (%)	91	91	88	84
ζ_H based on above estimates [$\zeta^2=2\ln\frac{\mu}{x_{50}}$]	0.32	0.32	0.29	0.31

CONDITIONAL FAILURE PROBABILITY – FRAGILITY

Before addressing the earthquake reliability problem, the more mundane reliability of structures under dead and live loads only is briefly reviewed to expound on the basic relations in reliability calculations.

Basic Reliability Relations (Dead and Live Loads)

Reliability analysis starts with the statistics of loads and resistances, such as means and standard deviations, the latter to quantify the uncertainties due to inherent variability, load modeling, structural analysis, and capacity estimates. These parameters are usually summarized as PDFs similar to those in Figure 4. Assuming that load, S, and resistance, R, are continuous statistically independent random variables, the probability of failure is given by (see, e.g., Ang and Tang [5])

$$P_F = P(R < S) = \int_0^{\infty} F_R(s) f_S(s) ds \quad (2)$$

At any given $S=s$, the area under R below s, where $r < s$, is $F_R(s)$. This is the conditional failure probability given s. The unconditional failure probability, P_F , is given by the product of $F_R(s)$ with the probability that s occurs, i.e., $f_S(s)ds$, integrated over all s. For the case of lognormally distributed R and S, the safety factor, $\theta = R/S$, is also a lognormal variate with the following parameters:

$$\lambda_\theta = \lambda_R - \lambda_S \quad \text{and} \quad \zeta_\theta^2 = \zeta_R^2 + \zeta_S^2$$

where ζ_R and ζ_S are the logarithmic standard deviations of the respective distributions, and

$$\lambda_R = \ln R_{50} \quad \text{and} \quad \lambda_S = \ln S_{50}$$

are the natural logarithms of the medians R_{50} and S_{50} , respectively. Equation 2 can now be reformulated in terms of the safety factor θ ; and failure would occur when $\theta < 1$, i.e., $R < S$. Thus,

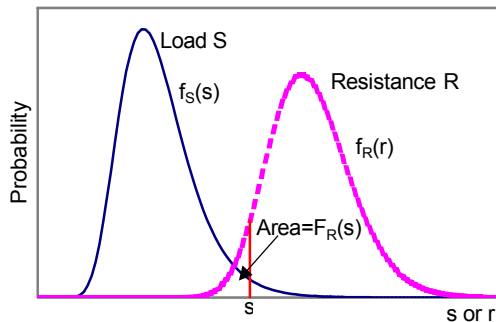


Figure 4. PDFs for load and resistance

$$P_F = \int_0^1 f_{\theta}(\theta) d\theta = F_{\theta}(1.0) \quad (3)$$

In terms of the median values of the distributions,

$$\lambda_{\theta} = \ln R_{50} - \ln S_{50} = \ln \frac{R_{50}}{S_{50}}$$

and therefore, from Equation 3,

$$P_F = F_{\theta}(1.0) = \Phi\left(\frac{\ln 1.0 - \lambda_{\theta}}{\zeta_{\theta}}\right) = \Phi\left(\frac{-\lambda_{\theta}}{\zeta_{\theta}}\right) = 1 - \Phi\left(\frac{\lambda_{\theta}}{\zeta_{\theta}}\right) = 1 - \Phi\left(\frac{\ln \frac{R_{50}}{S_{50}}}{\sqrt{\zeta_R^2 + \zeta_S^2}}\right) \quad (4)$$

The term in the last parenthesis is referred to as the reliability or safety index, β :

$$\beta = \frac{\lambda_{\theta}}{\zeta_{\theta}} = \frac{\ln \left(\frac{R_{50}}{S_{50}}\right)}{\sqrt{\zeta_R^2 + \zeta_S^2}} \quad (5)$$

And, thus, alternatively,

$$P_F = 1 - \Phi(\beta) \quad (6)$$

In Equations 4 and 5, ζ_S^2 incorporates the inherent variabilities of the concurrently acting loads, such as dead and live loads, as well as uncertainties in load modeling and response calculations. On the other hand, ζ_R^2 incorporates variabilities in material properties and capacity estimates. Partial load and capacity reduction factors used in building codes are derived from Equation 5 based on a preselected β . For a detailed evaluation of partial load factors see Hadjian, [6] and [7].

The AISC target reliability index for steel members is $\beta=2.6$. And, therefore, the failure probability for steel flexural members under dead and live loads, from Equation 6, is

$$P_F = 1 - \Phi(\beta) = 1 - \Phi(2.6) = 5 \times 10^{-3}$$

The point of this calculation is that a designer using the ASCE 7 specifications assures, knowingly or unknowingly, a failure probability of about 5×10^{-3} for a flexural member under dead and live loads. It should be emphasized that failure probability is not only a function of the median factor of safety, R_{50}/S_{50} , but also the uncertainty of loads and resistances, i.e., $\zeta = \sqrt{\zeta_R^2 + \zeta_S^2}$ (see Equation 4). The interaction of these parameters as they affect P_F can be visualized by referring to Figure 4: the relative positions of the PDFs determine the median factor of safety, and the ζ_i impact the extent of overlap of the distributions, and thus the reliability.

Conditional Failure Probability (Fragility) Under Earthquake Loads

Returning to the earthquake problem, although a designer is interested in a certain load intensity to complete his/her design (say, ground motion parameters at 10% in 50 years exceedance probability, as for Rare ground motion in Table 1), it should be noted that design to a specific ground motion parameter in terms of an exceedance probability, all by itself, is not a sufficient determinant of the problem at hand. Any one structure, in effect, is potentially exposed throughout its design life to *all* the possibilities of the occurrence of ground motion intensities at a site as characterized by a set of site specific seismic hazard curves as in Figure 1.

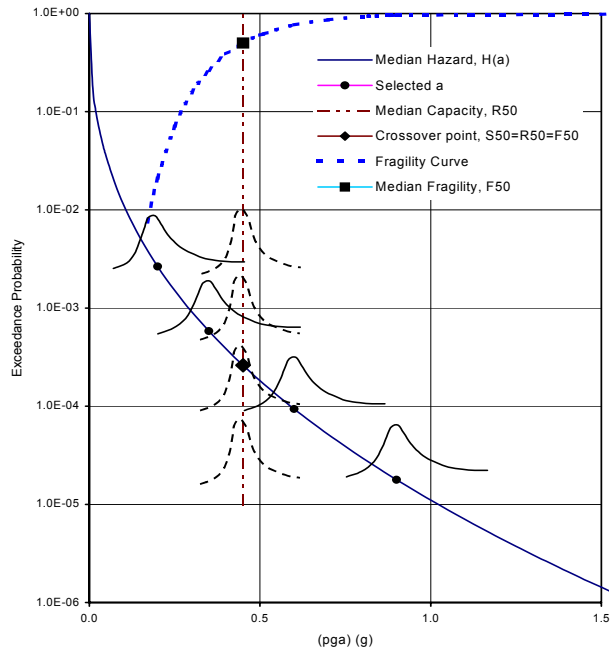


Figure 5 is a sketch used herein to expound on earthquake failure probability. In addition to the median hazard curve two sets of PDFs are shown at four selected exceedance probabilities, one representing the across-variability of the ground motion parameter (solid lines), and the other (dashed lines) the probability distribution of the resistance for a specified limit state. As shown, the PDF of the resistance is independent of the hazard and is the same for a given design. The PDF of the ground motion is anchored to the median, \tilde{a}_i , at each selected exceedance probability. The convolution of these load and resistance distribution functions (Equation 2), both assumed to be lognormally distributed with logarithmic standard deviations ζ_H and ζ_R respectively, would lead to a failure probability (Equation 4) for any selected ground motion exceedance probability, as in Figure 4. In this instance, however, the failure probabilities are *conditional* on the occurrence of ground motion \tilde{a}_i .

Figure 5. Seismic failure probability model and fragility curve

Repeating this convolution for all exceedance probabilities results in what is usually referred to as a fragility distribution, $F(a)$, with logarithmic standard deviation $\zeta = \sqrt{\zeta_H^2 + \zeta_R^2}$, shown in dashed line at the top left of Figure 5. When the load is small compared to the resistance (e.g., 0.2g vs 0.45g), the conditional failure probability is small (about 2×10^{-2} for $\zeta=0.4$). However, when the load is large (0.9g vs 0.45g), the conditional failure probability is very large (about 0.96). Simply stated, a fragility curve is the conditional failure probability of the system, given that median load level \tilde{a} occurs. Extensive studies [3] conclude that the fragility of structural systems and components can be assumed to be lognormally distributed (indirectly substantiating the lognormality of the across-variability discussed earlier), and thus characterized by their median values, F_{50} , and logarithmic standard derivations, ζ . As depicted in Figure 5, a proper fragility curve *must* consider the uncertainty in the ground motion parameter (across-variability), ζ_H . There are circumstances when this is not done and fragility curves are based solely on the

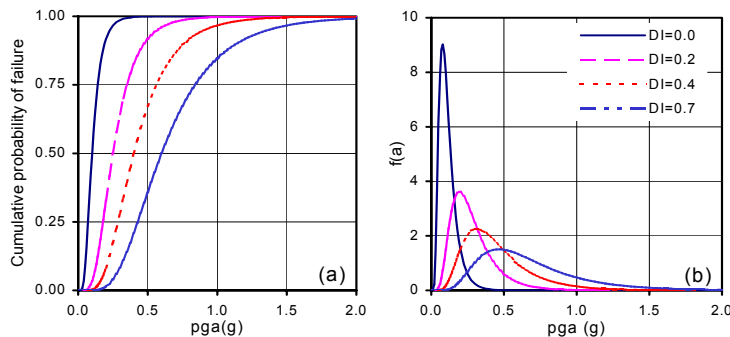


Figure 6. Idealized fragility curves for selected damage indices and $\zeta=0.5$: (a) CDF and (b) PDF

uncertainties of the structural resistance parameters. This is discussed below.

In Seismic Probabilistic Risk Assessment (SPRA) of nuclear power plants, the variability of the ground motion shown in Figure 1 is incorporated into the failure probability computations separately as part of the overall SPRA solution

scheme [3]. Consequently, even though the variability in SPRA fragility curves includes all other sources of uncertainty, to avoid double counting, the uncertainty in the ground motion is explicitly excluded when estimating SPRA fragility curves, i.e., $\zeta_{SPRA}^2 = \zeta^2 - \zeta_H^2 = \zeta_R^2$. In the present formulation, however, the ground motion uncertainty, ζ_H , must be accounted for at the outset.

A different $F(a)$ or its derivative $f(a)$ is required for each and every limit state as shown in Figure 6. Figure 6a shows a family of idealized fragility curves all with the same $\zeta=0.5$ for four different limit states. Limit states are characterized by damage indices (DI). $DI=0$ denotes elastic response, and $DI=1.0$ denotes total collapse. A $DI=0$ is usually used for the design of critical facilities such as nuclear power plants. A $DI=0.7$ would be appropriate when the design objective is only life-safety. Although ζ for each damage state is expected to be different, in Figure 6 the same $\zeta=0.5$ is used to highlight the impact of only DI on the shape of the distributions. The derivatives of these fragility curves are plotted in Figure 6b. For a detailed discussion of DIs see Hadjian [9].

RANDOMNESS AND UNCERTAINTY

In SPRA analysis, fragility is characterized as a set of curves at different “confidence” limits by separating the logarithmic standard deviation of the fragility, ζ , into its randomness and uncertainty components, ζ_r and ζ_u , such that $\zeta^2 = \zeta_r^2 + \zeta_u^2$. Randomness refers to inherent variabilities that are irreducible. It is the nature of the beast and there is not much that can be done about it. On the other hand, uncertainty refers to reducible variabilities that can be improved with more effort. The notion of separating variability into randomness and uncertainty, at least in practice, is an art more than a science.

The mechanics of separating randomness and uncertainty though is straightforward under the assumption of lognormal distributions. This is illustrated by the use of a numerical example, where $\zeta_r=0.3$, $\zeta_u=0.4$, and hence the combined $\zeta=0.5$. As shown in Figure 7a, the bold line is the fragility curve for the combined variability, ζ , and an arbitrary damage state with $F_{50}=0.9$. Using the *same* median of the total fragility curve, $a_{50}=0.9$, the distribution of the randomness component, CDF_p , can be obtained using ζ_r in the lognormal distribution. This curve is in effect the distribution when the uncertainty $\zeta_u=0$. To characterize the uncertainty, it is assumed that the median of the total fragility is lognormally distributed with logarithmic standard deviation, ζ_u ($=0.4$), and a set of lognormal CDF_u^p are calculated for selected “confidence” limits p , with “medians”, a_{50}^p , and logarithmic standard deviations, ζ_r . The a_{50}^p are

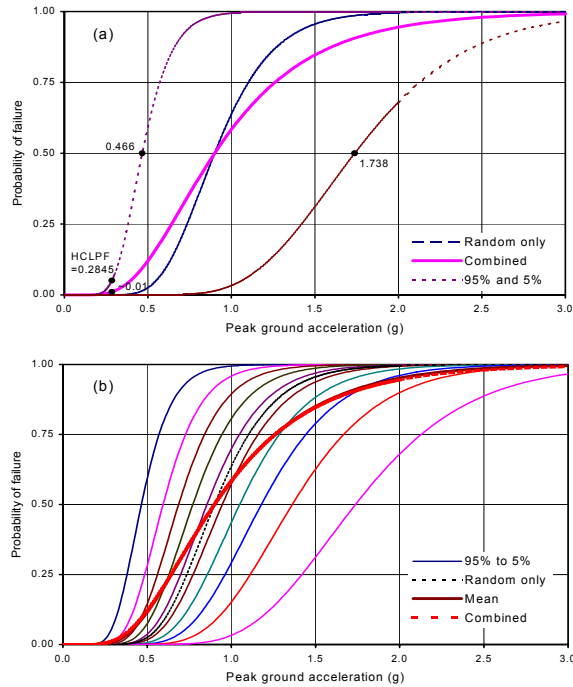
calculated from $\frac{x_p}{x_{50}} = e^{s_p \zeta}$. Since s_p for a_{50}^{50} is zero, $a_{50}^{50} \equiv a_{50}$, the median of the original total

fragility. For the 5% and 95% confidence limits, $s_p = \pm 1.645$, and hence the medians of these two

confidence limit distributions are $a_{50}^{0.95} = a_{50} e^{-1.645 \zeta_u} = 0.466$ and $a_{50}^{0.05} = a_{50} e^{+1.645 \zeta_u} = 1.738$.

Using these median values together with ζ_r , distribution functions at these confidence limits are calculated and plotted in Figure 7a (dashed lines). Other confidence limit distributions can be similarly calculated by the appropriate choice of $\pm s_p$. A set of such ten “equally-spaced” uncertainty distributions are shown in Figure 7b. At each pga the weighted sum of the probabilities (in this example the weights are all 0.1) is characterized as the “mean” fragility curve. This mean curve is also shown in Figure 7b,

together with the combined fragility curve with $\zeta = \sqrt{\zeta_r^2 + \zeta_u^2}$. These two curves almost coincide. As the number of the uncertainty confidence limit curves is increased, the weighted sum of the probabilities and the combined fragility curves tend to become identically the same. Also shown, for reference only (dashed lines), is the 50th percentile median fragility curve with $\zeta_r=0.3$.



What is achieved by the decomposition of ζ as in Figure 7? When risk decisions need to be made, it may be useful to know which component of the total variability, ζ_r or ζ_u , is the dominant contributor to the failure probability. This knowledge should lead the designer to take appropriate corrective actions. Additionally, statements like 95% confidence in a 5% probability of failure (commonly referred to in SPRA space as High Confidence of Low Probability of Failure, HCLPF) can be made. For this example the HCLPF can be calculated from

$$0.9 e^{-1.645 \times 0.4} \times e^{-1.645 \times 0.3} = 0.466 \times 0.610 = 0.2845g$$

where the first term is the median value of the 95% (high) confidence curve, and the second term, its 5% (low) exceedance probability. In general, therefore,

$$HCLPF = a_{50} e^{-1.645(\zeta_u + \zeta_r)} \quad (7)$$

Using the combined distribution with $\zeta=0.5$, the failure probability would, from Equation 4, be equal to

Figure 7. Example of confidence limits on failure probability for $\zeta=0.5$, $\zeta_r=0.3$ and $\zeta_u=0.4$: (a) 95% and 5%, (b) 95% to 5% in increments of 10%

$$P(X \leq b) = \Phi \left(\frac{\ln 0.2845 - \ln 0.9}{0.5} \right) = \Phi(-2.303) = 1 - \Phi(2.303) = 1 - 0.9894 = 0.0106$$

When $\zeta_r = \zeta_u$, for any value of these parameters, 95% confidence in a 5% probability of failure becomes identically equal to a $P_F = 0.01$. As ζ_r and ζ_u tend to differ the failure probability slightly increases as exemplified above. Thus, for reasonably close ζ_r and ζ_u , HCLPF approximately equals a $P_F \approx 0.01$. From a practical point of view, a statement that $P_F = 0.01$ is more useful and meaningful than the rather convoluted statement, however mathematically correct, of a 95% confidence in a 5% probability of failure. Similarly, a 90% confidence in a 10% probability of failure is tantamount to a $P_F \approx 0.035$ for similar valued ζ_r and ζ_u . Whether, for example, $\zeta_u = 0.24$ and $\zeta_r = 0.55$, or $\zeta_u = 0.55$ and $\zeta_r = 0.24$, HCLPF = 0.245, and the associated P_F from the combined fragility curve is $P_F = 0.015$. The fact that in the second case the uncertainty is much larger (0.55) than in the first case (0.24) has no bearing on HCLPF. Thus HCLPF, or any other confidence level in a low probability failure designation, is simply a mathematical manipulation without any intrinsic use. Failure probability P_F computed from the combined fragility curve is a more direct and useful measure for making design decisions.

UNCONDITIONAL FAILURE PROBABILITY – P_F

To calculate the unconditional failure probability, P_F , $F(a)$ must be multiplied by the corresponding probability of the occurrence of \ddot{a} , viz., $h(a)da$, where $h(a)$ is the PDF of the median hazard (e.g., Figure 2c), and then summed over all occurrences of \ddot{a} . Thus (the carrot is dropped for simplicity),

$$P_F = \int_0^{\infty} F(a) h(a) da \quad (8)$$

Alternatively (Ang and Tang [5]), P_F can be formulated with respect to $f(a)$, giving

$$P_F = \int_0^{\infty} [1-H(a)] f(a) da = \int_0^{\infty} \hat{H}(a) f(a) da \quad (9)$$

where $H(a)$ is the CDF of the hazard, and $\hat{H}(a)$, its Complementary CDF, is the median hazard curve.

Approximate Solution of Equation 9

In general, Equation 9 must be integrated numerically. However, making one simplifying assumption, Equation 9 can be integrated in closed form resulting in a simple relation. Assuming a lognormally distributed fragility curve with median F_{50} and variance $\zeta^2 = \zeta_R^2 + \zeta_H^2$, Equation 9 can be written as

$$P_F = \int_0^{\infty} \hat{H}(a) \frac{1}{a\zeta\sqrt{2\pi}} e^{-\frac{\left(\ln \frac{a}{F_{50}}\right)^2}{2\zeta^2}} da \quad (10)$$

Defining $M = \ln F_{50}$ and $x = \ln a$, and appropriately changing the limits of the integration ($a = e^x$ and $da = e^x dx$), Equation 10 can be written as

$$P_F = \int_{-\infty}^{\infty} \hat{H}(a) \frac{1}{\zeta\sqrt{2\pi}} e^{-\frac{(x-M)^2}{2\zeta^2}} dx \quad (11)$$

To perform the closed-form integration of Equation 11, Kennedy and Short [10] approximate the hazard curve by

$$H_a = K_1 a^{-K_H} \quad (12)$$

where K_1 is a constant and K_H is a slope parameter defined as

$$K_H = \frac{1}{\log(A_R)} \quad (13)$$

wherein A_R is the ratio of ground motion intensities along the hazard curve corresponding to a ten-fold reduction in exceedance probability. In effect, Equation 12 linearizes the hazard curve on a log-log plot using two points on the hazard curve separated by a decade in exceedance probability. The appropriateness of this approximation is explored subsequently.

Substituting Equation 12 into Equation 11 results in

$$P_F = \frac{K_1}{\zeta\sqrt{2\pi}} \int_{-\infty}^{\infty} e^{-K_H x} e^{-\frac{(x-M)^2}{2\zeta^2}} dx \quad (14)$$

Performing the above integration (e.g., Elishakoff [11]), the failure probability is obtained as

$$P_F = K_1 e^{-K_H M} e^{\frac{(K_H \zeta)^2}{2}}$$

Re-substitution of $M = \ln F_{50}$ or $F_{50} = e^M$ into the above equation results in

$$P_F = K_1 F_{50}^{-K_H} e^{\frac{(K_H \zeta)^2}{2}} \quad (15)$$

Defining H_D as the annual frequency of exceedance of the median Design Basis Earthquake (DBE)

ground motion intensity (e.g., $H_D=4 \times 10^{-4}$ as in the USGS seismic hazard maps), from Equation 12

$$K_1 = H_D (DBE)^{K_H} \quad (16)$$

Substituting Equation 16 into Equation 15 gives the final algebraic expression for P_F :

$$P_F = \frac{H_D e^{\frac{(K_H)^2}{2}}}{(F_{50}/DBE)^{K_H}} \quad (17)$$

where F_{50}/DBE , termed herein as *design factor*, DF_{50} , is the ratio of the median of the applicable *in-situ* limit state fragility to the design ground motion intensity at H_D , in same units. The in-situ median fragility is related to the “as-built” condition of the structure and depends on several factors such as response analysis models and methods, any safety factors used in design, implicit design conservatism, redundancy, quality in design, materials and construction, etc.. The actual code nominal design capacity, R_n , can be backed out from the required in-situ median fragility as described in Hadjian [12].

Evaluation of the Approximate Solution (Equation 17)

In order to evaluate the approximate solution, a set of hazard curves are represented analytically as

$$\log \hat{H}(a) = ba^n \quad (18)$$

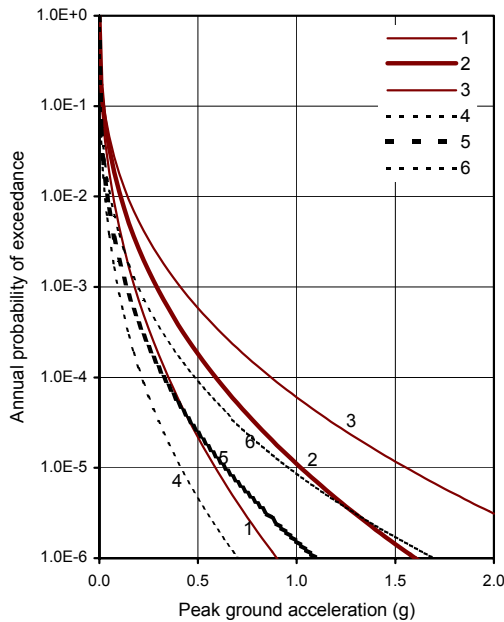


Figure 8. Idealized High (1, 2, 3) and Low (4, 5, 6) hazard curves

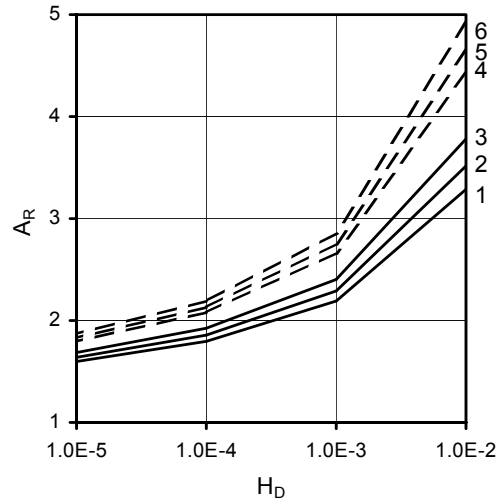


Figure 9. Variation of A_R along hazard curves 1-6

where b and n are constants. The purpose of an analytical representation of the hazard curve is to facilitate the numerical integration of Equation 10 for several $\hat{H}(a)$. Figure 8 shows a family of pga hazard curves based on Equation 18 in two sets. The full line Curves 1, 2 and 3 are considered to be representative of high seismicity hazard curves, and the dashed line Curves 4, 5 and 6 are considered to be representative of low seismicity hazard curves. The b and n values for all six hazard curves are listed in Table 3 (together with their A_R and K_H values calculated at $H_D=10^{-4}$). Figure 9 is a plot of the A_R (calculated at the midpoint of the decade for all six hazard curves of Figure 8) as a function of H_D . The

wide range spanned by Curves 1 and 3, and Curves 4 and 6 qualify these sets of curves as a reasonable basis for a generalized evaluation of Equation 17.

Table 3. Characteristics of the six hazard curves of Figure 8

		High Seismicity			Low Seismicity		
Curve #		1	2	3	4	5	6
b		-6.28	-4.96	-4.22	-6.78	-5.81	-5.06
n		0.429	0.406	0.384	0.343	0.333	0.321
$H_D=10^{-4}$	A_R	1.80	1.86	1.92	2.08	2.13	2.19
$H_D=10^{-4}$	K_H	3.93	3.72	3.52	3.15	3.05	2.94

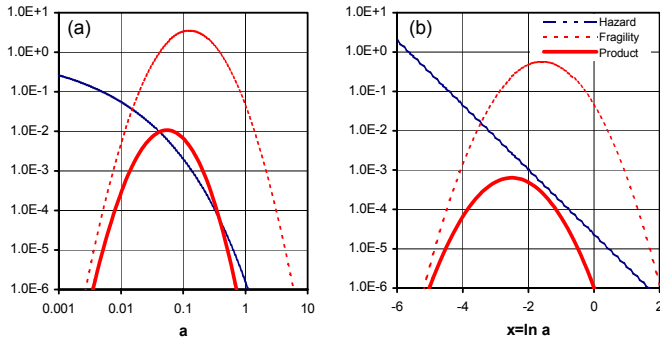
Figure 10 shows a sample of the solution of Equation 10 by using

- (a) the analytical form of the hazard curve (Equation 18), and
- (b) the linearized (ln a vs log P_F) hazard curve (Equation 12).

The parameters used in this example are: Curve 2 of Figure 8,, $\zeta=0.4$, $F_{50}=0.582$, and $H_D=10^{-3}$. At $H_D=10^{-3}$, $DBE=0.291$, $A_R=2.29$, $K_H=2.78$, and $DF_{50}=F_{50}/DBE=2.0$. A_R is calculated for the decade from $10^{-3.5}$ to $10^{-2.5}$ instead of from the decade below (10^{-4} to 10^{-3}), as recommended in [10].

	Hazard	Fragility	
a) Equation 14	$K_1 e^{-K_H x}$	$\frac{1}{\zeta\sqrt{2\pi}} e^{-\frac{(x-M)^2}{2\zeta^2}}$	The three curves shown in Figure 10 are the hazard (dashed line), the fragility density function (dotted line), and the product of the two parameters (full line). The area under the product curve is therefore, from Equation 9, the failure probability, P_F . A direct comparison of curves as in Figures 10 a and b is not possible because the independent variables are different (a and $x=\ln a$). The basic parameters in
b) Equation 10	$H(a) = 10^{ba^n}$	$\frac{1}{a\zeta\sqrt{2\pi}} e^{-\frac{(\ln \frac{a}{F_{50}})^2}{2\zeta^2}}$	

Equations 14 and 10 have been apportioned for plotting purposes as shown above left. The main difference in the two solutions is the curvature of the hazard curves (dashed lines). The hazard curve in Figure 10a is the actual Curve 2 of Figure 8 (in log-log plot), whereas that in Figure 10b is a linear replacement. The resulting failure probabilities (area under the product curve—full line) are given below (Cases a and b). As is to be expected from Figure 10b, Equation 14 will result in a larger P_F because the concavity of the true hazard curve is lost by its linearization, and hence the product with the fragility PDF will be larger than its counterpart in Figure 10a.



The K_H value used in these examples is calculated at the vicinity of $H(a) = 10^{-3}$, from the A_R for the decade from $10^{-3.5}$ to $10^{-2.5}$. If the decade from 10^{-4} to 10^{-3} (i.e., from below) were

Figure 10. Comparison of two characterizations of hazard curves, Equations 18 and 12

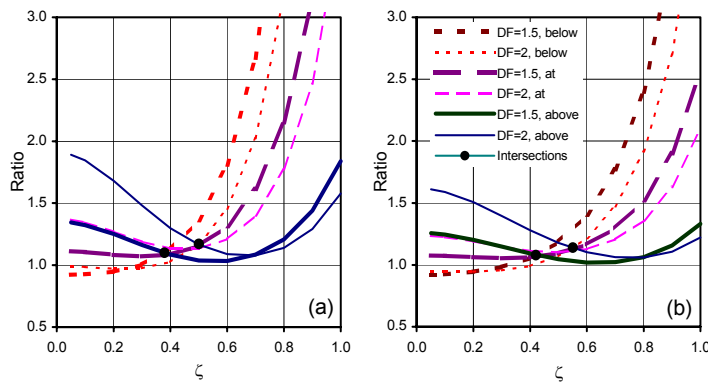
Case		$\zeta = 0.2$	$\zeta = 0.4$	Comments
(a)	Eqs. 10 and 18	1.34×10^{-4}	2.38×10^{-4}	
(b)	Equation 14	1.70×10^{-4}	2.70×10^{-4}	A_R at vicinity of H_D ($K_H=2.78$)
(c)	Equation 14	1.30×10^{-4}	2.45×10^{-4}	A_R from below H_D ($K_H=3.25$)

to be used, A_R would equal 2.03 instead of 2.29, and K_H would equal 3.25 instead of 2.78. For $\zeta = 0.4$,

from Equation 17, $P_F = 10^{-3} \times \frac{e^{0.5(3.25 \times 0.4)^2}}{2^{3.25}} = 2.45 \times 10^{-4}$ instead of 2.70×10^{-4} , and for $\zeta = 0.2$, P_F

would equal 1.30×10^{-4} instead of 1.70×10^{-4} . As compared in the above table, these results (Case c) are closer to those obtained directly by use of Equations 10 and 18 (Case a). Although the choice of A_R calculation at the vicinity of H_D makes conceptual sense (in that K_H is analogous to the slope of the hazard curve at H_D), it seems that the errors due to the linearization of the hazard curve and the calculation of A_R from the decade below H_D counterbalance each other to produce the above encouraging results. Based on similar evaluations, A_R is invariably calculated in current practice from the decade below H_D [10].

However, these evaluations are based on small ζ (≤ 0.4 , as in the above example). When the across-variability of the hazard curve, ζ_H , is considered in fragility calculations, as it should be, ζ approaches to 1.0, and the calculation of P_F by Equation 17 and A_R from below results in significant overestimates of the failure probability as shown in Figure 11, where the ratio of P_F using Equation 17 to P_F based on the



integration of Equation 10 is shown as a function of ζ for three different methods of computing A_R for use in Equation 17. These are characterized as “below”, “at” and “above”. “below” and “at” characterizations of A_R were just discussed. “above” refers to the calculation of A_R based on the decade above H_D . For $H_D=10^{-3}$, A_R from above would be based on the ground motion parameter ratio from $H_D=10^{-3}$ to $H_D=10^{-2}$. All three characterizations are shown in Figure 11 for $H_D=10^{-3}$ and $DF_{50}=1.5$ and 2.

Figure 11. Ratio of approximate to correct P_F for three definitions of A_R and $DF_{50}=1.5$ and 2.0 (a) hazard Curve 2, (b) hazard Curve 5

As expected from the earlier discussion, for small ζ the prediction of P_F for A_R from below is excellent. However, for large ζ the overestimation increases exponentially. For $DF_{50}=1.5$, $\zeta=0.92$ gives a ratio of 10, an order of magnitude overestimate of P_F . At $\zeta=0.85$ the overestimation is three times. Rather surprisingly, for large ζ , A_R from above gives the best results. This trend can be explained with reference to Figure 10. As ζ increases the fragility curves (dotted lines) spread out and the straight line extension of the hazard curve to the left (Figure b) gets engaged, and thus contributes a much larger portion to the total P_F than the true hazard curve would (which tends to flatten out to the left). It should be observed that on the right-hand side of the figures, the spreading out of the fragility curves for large ζ is not critical, since the hazard curves become more than an order of magnitude smaller than H_D where the A_R are calculated.

Thus, the contribution of any hazard curve to P_F outside of a reasonable fragility band, say at 1% of its mode value, is therefore minimal. This suggests that the shape of hazard curves slightly beyond H_D is not critical to the calculation of P_F . In other words, the right-side “tail” of the hazard PDF is not critical to the estimation of P_F . This observation is important since the uncertainty estimates of hazard curves for very small ground motion exceedance probabilities tend to become speculative. Recall that the fragility curve in Figure 5 is predicated on a constant ζ_H at all exceedance probabilities.

Returning to Figure 11, it is observed that the appropriate estimation method of A_R where error would be minimum, (i.e., the bottom envelope of the curves) depends on ζ . For the example of Figure 11, the ζ boundary between A_R^b (from below) and A_R^a (from above) that give the least error are as follows (dots):

	High Hazard	Low hazard
DF ₅₀ =1.5	$A_R^b < 0.38 \leq A_R^a$	$A_R^b < 0.42 \leq A_R^a$
DF ₅₀ =2.0	$A_R^b < 0.50 \leq A_R^a$	$A_R^b < 0.55 \leq A_R^a$

An average ζ boundary at about $\zeta_b=0.45$ can be established. Thus, for $\zeta_b \leq 0.45$ best results would be obtained by calculating A_R from below, and for $\zeta_b \geq 0.45$ best results would be obtained by evaluating A_R from above. However, in practical applications $\zeta \geq 0.3$, if not ≥ 0.4 . Under this circumstance, the above complexity of defining boundaries can be eliminated, and A_R can be calculated for all ζ and all DF₅₀ from the decade above H_D . This is contrary to current practice, which is based on small ζ used in SPRA [10].

P_F as a ratio of H_D

It should be noted from Equation 17 that the design level exceedance probability, H_D , and the failure probability, P_F , can be significantly different (numerically) depending on the slope parameter of the hazard curve, K_H , the in-situ median fragility, F_{50} , and the logarithmic standard deviation, ζ . This point, illustrated in Figure 12, where A_R are calculated from above, needs to be emphasized. Figures 12 b-d show plots of the P_F/H_D ratio as a function of the design factor, F_{50}/DBE , based on the idealized seismic hazard Curve 2 (for Western US – WUS) and Curve 5 (for Eastern US – EUS) repeated in Figure 12a. The use of these specific median hazard curves is immaterial to the issues being discussed here. Multiplying the design factor by the DBE determines the required in-situ median fragility, F_{50} .

P_F/H_D depends, in a rather complex manner, on the variation of K_H along any one of the hazard curves. And, for any ground motion design basis exceedance probability (each one of the curves), different failure probabilities are obtained than the respective exceedance probabilities of the design basis earthquake motions, H_D , as a function of both the design factor and ζ . As H_D decreases (or return period increases) the impact of the design factor on the P_F/H_D ratio increases dramatically, and could vary by orders of magnitude (Figure 12 ordinate is logarithmic). A comparison of Figures 12b and 12c (same ζ), shows that P_F/H_D is more sensitive to changes in the design factor in the WUS relative to EUS. And a comparison of Figures 12c and 12d shows a significant dependence of P_F/H_D on ζ .

Based on the above results it should become obvious that simply designing to a specific annual exceedance probability of the ground motion, say 10% in 50 yr, is misleading: it does not provide any information on failure probability. For example, if designing to a 500 yr return period ground motion is meant to achieve a failure probability of 10% in 50 yr, the required design factors, from Figure 12 (dotted line), should be 1.7 for EUS hazard and $\zeta=0.8$ (Figure b), 1.9 for WUS hazard and $\zeta=0.8$ (Figure c), and 1.4 for WUS hazard and $\zeta=0.6$ (Figure d). This and related issues have been belatedly recognized in FEMA 350 [13], where an alternative method is used to estimate the “confidence” level that the specified performance reliability at a specified limit state (Immediate Occupancy or Collapse Prevention) for a given design has been attained. Cornell et al. [14] give the probabilistic basis for this corrective action.

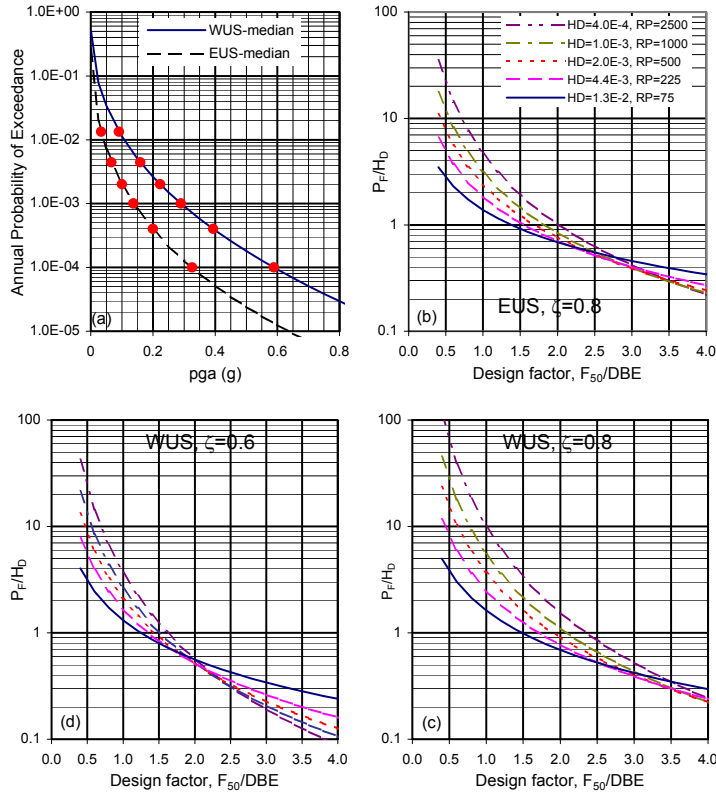


Figure 12. Comparison of P_F/H_D vs F_{50}/DBE (b, c and d) for WUS and EUS hazard curves (a), selected ζ and five H_D

increasing seismicity (a regional effect), and, for a given hazard curve, increases with decreasing exceedance probability, or increasing design ground motion (a design condition): K_H increases with increasing design level of structures, from ordinary to essential and to critical facilities.

Based on Figure 13 the following observations are made: (1) When $\zeta \neq 0$, a $DF_{50} > 1.0$ is required to achieve the design failure specification, $P_F = H_D$.

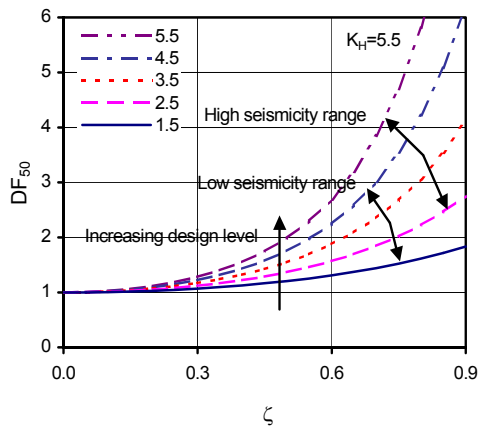


Figure 13. Impact of ζ on K_H and DF_{50}

$P_F = H_D$
On the presumption that the selection of the specific ground motion return periods in Table 1 is to achieve comparable failure probabilities, the impact of ζ and K_H on DF_{50} is explored below. Setting $P_F = H_D$, Equation 17 reduces to

$$e^{\frac{(K_H \zeta)^2}{2}} = (DF_{50})^{K_H}$$

Taking the natural logarithm of this relation gives

$$\frac{(K_H \zeta)^2}{2} = K_H \ln DF_{50} \quad \text{or} \quad \ln DF_{50} = \frac{K_H \zeta^2}{2}$$

DF_{50} are calculated for selected K_H and a broad range of ζ , and the trends shown in Figure 13. As discussed earlier, the determination of the K_H parameter of hazard curves for use in Equation 17 is not a simple decision. To avoid this controversial issue, K_H is used as an independent parameter, varying from 1.5 to 5.5. K_H , in general, increases with

(2) The dependence of DF_{50} on ζ becomes more significant as K_H increases. DF_{50} grows faster with ζ as K_H gets larger. For example, a change of ζ from 0.6 to 0.7 for $K_H = 5.5$ increases DF_{50} from 2.7 to 3.9, and for $K_H = 1.5$, the increase in DF_{50} is only from 1.31 to 1.44. Thus, in high seismicity regions and for increasingly important structures, the selection of ζ becomes a more critical design decision than in low seismicity regions and for less important structures. Thus, a design load specification, particularly in high seismicity regions, that does not explicitly include a consideration of ζ is quite useless. (3) Assuming that ζ is adequately determined and appropriately considered, DF_{50} becomes a function of K_H . Thus, design load criteria to achieve the same reliability must be different from region to region.

The use of the same load factors for the whole country, as for example used in dead and live load combinations, would lead, in a relative sense, to underdesigns in high seismicity regions and overdesigns in low seismicity regions. Earthquake design load factors must therefore be regional. This is an issue that building code framers need to consider.

CONCLUSIONS

The current practice of designing structures to a specified return period of a ground motion parameter does not translate into any useful estimate of failure probability. This is so simply because any one structure, in effect, is potentially exposed, throughout its design life, to *all* the possibilities of the occurrence of ground motion intensities at a given site as characterized by a set of site-specific seismic hazard curves. A simple failure probability model is derived with certain constraints on the calculation of A_R . Based on this model the following conclusions are made: P_F is related to H_D in a rather complex and significant manner as a function of both DF_{50} and ζ . The across-variability parameter, ζ_H , has a significant impact on reliability, and must be explicitly included in design. For the same ζ , P_F/H_D is more sensitive to changes in the design factor in the WUS relative to EUS. A $DF_{50} > 1.0$ is *required* to achieve the design failure specification, $P_F = H_D$. In high seismicity regions and for increasingly important structures, the selection of ζ becomes a more critical design decision than in low seismicity regions and for less important structures. The use of the same load factors for the whole country, as for example used in dead and live load combinations, would lead, in a relative sense, to underdesigns in high seismicity regions and overdesigns in low seismicity regions.

REFERENCES

1. Poland CD "SEAOC VISION 2000: A comprehensive approach towards the development of performance-based seismic design standards." Proc 63rd SEAOC Annual Convention, 1994, 265-8.
2. SSHAC "Recommendations for probabilistic seismic hazard analysis: guidance on uncertainty and use of experts." Seismic Safety Hazard Analysis Committee, NUREG/CR-6372, Washington, DC.
3. EPRI "Methodology for developing seismic fragilities." EPRI TR-103959, Menlo Park, Calif., 1994.
4. Ang A H-S and Tang WH "Probability concepts in engineering planning and design, Vol. I-Basic Principles." John Wiley & Sons, New York, 1975.
5. Ang A H-S and Tang WH "Probability concepts in engineering planning and design, Vol. II: Decision, Risk, and Reliability." John Wiley & Sons, New York, 1984.
6. Hadjian AH "A basic limitation of partial load factors", Proc (CD-ROM) 8th Joint Specialty Conf on Probabilistic Mechanics and Structural Reliability, Univ. of Notre Dame, July 2000.
7. Hadjian AH "Issues with partial load factors", Proc (CD-ROM) 8th Int'l Conf. on Structural Safety and Reliability, ICOSSAR 2001, Newport Beach, CA, June 2001, Balkema, Rotterdam.
8. Ellingwood B, Galambos TV, MacGregor JC and Cornell CA "Development of a probability based load criteria for American National Standard A58." NBS Special Publication 577, 1980.
9. Hadjian, AH "A general framework for risk-consistent seismic design." Earthquake Engng and Struct Dyn, 2002, 31:601-26.
10. Kennedy RP and Short SA "Basis for seismic provisions of DOE-STD-1020." UCRL-CR-11478 and BNL-52418, 1994.
11. Elishakoff I "Probabilistic methods in theory of structures." John Wiley & Sons, New York, 1983.
12. Hadjian AH "Extension of seismic zonation maps for design at any preselected failure probability." Proc (CD-ROM) 12th WCEE, Paper No. 1811/8/A, 2000.
13. FEMA 350 "Recommended seismic design criteria for new steel moment-frame buildings." Report No. FEMA-350, SAC Joint Venture, Federal Emergency Management Agency, Washington, 2000.
14. Cornell CA, Jalayer F, Hamburger RO, Foutch DA "Probabilistic basis for 2000 SAC/FEMA steel moment frame guidelines." ASCE J of Struct Engng, 2002, 128(4):526-33.